Biosensors and Bioelectronics 127 (2019) 167–173

Contents lists available at ScienceDirect

Biosensors and Bioelectronics

journal homepage: www.elsevier.com/locate/bios

An enzyme-free electrochemiluminescence biosensor for ultrasensitive assay of *Group B Streptococci* based on self-enhanced luminol complex functionalized CuMn-CeO_2 nanospheres

Jiaji Ling[a,1], Min Zhao[b,1], Fengjiao Chen[a], Xiaoyan Zhou[b], Xiaosong Li[c], Shijia Ding[b], Hua Tang[a,*]

[a] Key Laboratory of Molecular Biology for Infectious Diseases (Ministry of Education), Institute for Viral Hepatitis, Department of Infectious Diseases, The Second Affiliated Hospital, Chongqing Medical University, Chongqing 400016, China
[b] Key Laboratory of Clinical Laboratory Diagnostics (Ministry of Education), College of Laboratory Medicine, Chongqing Medical University, Chongqing 400016, China
[c] The Center for Clinical Molecular Medical Detection, The First Affiliated Hospital of Chongqing Medical University, Chongqing 400016, China

ARTICLE INFO

Keywords:
CuMn-CeO_2-PEI-luminol
Electrochemiluminescence
MNAzyme
Intramolecular co-reaction
Group B Streptococci

ABSTRACT

Herein, a novel and pragmatic electrochemiluminescence (ECL) biosensing method was developed for ultrasensitive and specific detection of *Group B Streptococci* (GBS) by combining self-enhanced luminol complex functionalized CuMn-CeO_2 (CuMn-CeO_2-PEI-luminol) with MNAzyme-mediated target-recycling amplification. First, the efficient self-enhanced PEI-luminol luminophore was prepared by combining PEI co-reactant with luminol in one molecular, which shortened electron transfer distance and enhanced ECL signal. And CuMn-CeO_2 was applied to load a large number of PEI-luminol and strengthen luminous efficiency of luminol by the high catalytic activity toward H_2O_2 oxidation. Then, target-driven MNAzyme system was used to realize the circulation of GBS nucleic acid sequence, producing plentiful triggers to initiate the hybridization reaction on the surface of electrode. The developed enzyme-free ECL biosensor showed ultra-sensitivity for target DNA detection with detection limits of 68 aM (synthetic DNA) and 5×10^2 CFU mL^{-1} (genomic DNA extracted from GBS strain). More importantly, this biosensor was successfully applied for detection of genomic DNA of GBS extracted from clinical vaginal/anal swabs as low as 320 copies. Thus, this proposed strategy might be an pragmatic ECL platform for ultrasensitive and specific detection of GBS in clinical vaginal/anal swabs.

1. Introduction

Electrochemiluminescence (ECL), caused by an energetic electron-transfer reaction at the electrode surface between electrochemically generated species with the light emission (Zhao et al., 2017, 2016), has been widely applied as a powerful tool in areas of clinical diagnosis (Zhou et al., 2018), forensic identification (Mao et al., 2011) and food analysis (Hao and Wang, 2016). In variety of ECL systems, the luminol or its derivatives-based ECL system is commonly used in bioassays owing to its nontoxicity, inexpensiveness, chemical and thermal stability, and high luminescent efficiency (Mayer et al., 2018). It is well-known that the introduction of co-reactants to ECL luminophores, such as H_2O_2, can significantly improve the luminous efficiency (Ke et al., 2018). However, such ECL co-reaction by intermolecular interaction has some shortcomings of the long electron transfer path and massive energy loss, which restricts the luminous efficiency enhancement (Danis et al., 2018; Liang et al., 2018). Recently, a new ECL co-reaction pattern through intramolecular interaction has been developed based on self-enhanced luminophores simultaneously containing luminophore and its co-reactive group in one molecular structure, which possesses high luminous efficiency and stability (Jiang et al., 2016; Wang et al., 2015, 2016c). Polyethylenimine (PEI), as a biocompatible polymer with massive primary and tertiary amine (Zhao et al., 2015), is a potential efficient co-reactant of luminol-based ECL system which can bond with luminol easier than other molecules for its relatively active amino groups. Here, we combine the PEI with luminol to prepare an efficient and stable self-enhanced ECL luminophore (PEI-luminol complex) for strong ECL light radiation.

Over the past years, metal oxides with special surface mixed-valence properties have attracted increasing attention in biosensors construction due to their excellent biocompatibility, unique electrical and catalytic properties (Kuo et al., 2014; Yang et al., 2016). Cerium oxide (CeO_2), one of the rare earth metal oxides, simultaneously exists Ce^{3+} and Ce^{4+} oxidation states on the lattice surface (Wang et al., 2016a; Xu and Wang, 2012). This redox pair Ce^{3+}/Ce^{4+} of CeO_2 can switch

* Correspondence to: 1 Yi Xue Yuan Road, Chongqing 400016, China.
E-mail address: tanghua86162003@cqmu.edu.cn (H. Tang).
[1] These authors have contributed equally to this work.

https://doi.org/10.1016/j.bios.2018.12.012
Received 1 October 2018; Received in revised form 7 December 2018; Accepted 10 December 2018
Available online 13 December 2018
0956-5663/

rapidly and reversibly to form O vacancies, endowing high catalytic properties and electron-transfer rate (Wang et al., 2016b). Later, Stroppa's group elaborated that the doping of Gd into CeO_2 nanocrystals could improve O vacancies, resulting in the significant increase of the catalytic performance (Stroppa et al., 2014). Also, Mandal's group demonstrated that the catalytic activity of CeO_2 was significantly improved by doping Sm (Mandal et al., 2016). Inspired by the above-mentioned cases, Cu/Mn dual elements are doped into CeO_2 nanocrystals to obtain high catalytic performance of Cu/Mn double-doped CeO_2 nanocomposites (CuMn-CeO_2). Besides, the prepared CuMn-CeO_2 nanocomposites with large specific surface area can also act as a preeminent nanocarrier in ECL biosensing applications.

To further improve the detection sensitivity of the ECL bioanalysis assay, various nucleic acid-based signal amplification strategies have been developed (Yan et al., 2016), especially the enzyme free nucleic acid amplification. For example, the catalyzed hairpin assembly (CHA) (Zhang et al., 2018), hybridization chain reaction (HCR) (Zhang et al., 2017) and entropy-driven catalysis (Zhang et al., 2007), etc. Multi component DNAzyme (MNAzyme), as one kind of DNAzyme, possesses some advantages of economic cost, mild reaction conditions, strong stability and simple operation comparing to the biologic enzymes, showing specific ability to cleave the substrates (Mokany et al., 2010; Wang et al., 2011). Thus, in this work, target-driven MNAzyme is designed to achieve target-recycling signal amplification without the use of enzymes.

Group B Streptococci (GBS) as an important pathogen at perinatal stage can cause neonatal sepsis and even death. Thus, early screening of GBS is of vital importance in clinical cases (Johri et al., 2006). Here, based on the self-enhanced PEI-luminol functionalized CuMn-CeO_2 signal tag and MNAzyme-mediated target-recycling amplification strategy, an enzyme-free ECL biosensor for ultrasensitive detection of GBS was constructed in this work. The principle of the proposed ECL biosensing platform was depicted in Scheme 1. First, CuMn-CeO_2 nanomaterials prepared by hydrothermal method were encapsulated with PEI to make the CuMn-CeO_2 endow mass amino groups, which further cross-linked with luminol via glutaraldehyde (GA) to obtain the self-enhanced PEI-luminol functionalized CuMn-CeO_2 nanocomposites (CuMn-CeO_2-PEI-luminol). Then the resultant CuMn-CeO_2-PEI-luminol was served as tracing tag by immobilizing signal probe (SP) to obtain the CuMn-CeO_2-PEI-luminol-SP (abbreviated as SP bioconjugates) (Scheme 1A). Meanwhile, the thiol-modified capture probe (CP) was assembled on the Au modified electrode through Au-thiol bond. In the presence of target DNA, the two partzymes co-recognized with target DNA to form a stable active MNAzyme which further combined with hairpin (HP) substrate for cleavage with the assistant of Mg^{2+} cofactor. After the cleavage reaction, the HP substrate was cleaved into two segments (trigger fragment and the other part), releasing the activated MNAzyme for next cycle. The obtained trigger fragment as a mediator hybridized with SP bioconjugates and CP, making the SP bioconjugates assembled onto the modified electrode (Scheme 1B). When the modified electrode was detected in the test solution containing H_2O_2, a high ECL signal was achieved, attributing to the intramolecular enhancing of efficient PEI-luminol luminophore and the intermolecular enhancing of highly catalytic CuMn-CeO_2 toward H_2O_2 oxidation (Scheme 1C). In this work, the novel self-enhanced luminol complex functionalized CuMn-CeO_2-based ECL biosensing strategy could not only realize highly sensitive and efficient detection of target DNA but also present a novel and pragmatic platform toward ultrasensitive detection of GBS in clinical samples. It would be a potential tool for general application in nucleic acid analysis and clinical diagnosis.

2. Experimental

2.1. Reagents and materials

Cerium nitrate hexahydrate ($Ce(NO_3)_3{\cdot}6H_2O$), copper chloride ($CuCl_2{\cdot}2H_2O$), manganese chloride ($MnCl_2$), polyvinylpyrrolidone (PVP), ethylene glycol (EG), luminol (98%) and all DNA oligonucleotides were purchased from Sangon Biotech. (Shanghai, China). The detailed sequences were listed in Table S1. Polyethylenimine (PEI, 50 wt% in water), 6-mercapto-1-hexanol (MCH), N-(3-dimethylaminopropyl)-N-ethylcarbodiimidehydrochloride (EDC) and N-hydroxysuccinimide (NHS) were bought from Sigma Aldrich (St. Louis, MO, USA). Glutaraldehyde (50%, GA), salmon sperm DNA and Bacterial Genomic DNA Extraction Kit were purchased from Solarbio Inc. (Beijing, China). The *Group B Streptococus* (GBS) Nucleic Aid Detection Kit (Fluorescent PCR) was purchased from BioChain Technology Co., Ltd. (Beijing, China). The surface immunogenic protein gene of GBS (GenBank Accession no. 1012782) exists in all GBS was used as target. MNAzyme buffer (pH 7.4) contained 40 mM Tris, 0.28 nM NaCl, 10 mM KCl, and 30 mM $MgCl_2$. Phosphate buffered solution (PBS, 0.1 M, pH 7.4) was prepared by mixing 0.1 M KCl, 0.1 M Na_2HPO_4, and 0.1 M KH_2PO_4, which was employed in this research. Deionized water obtained from a Millipore water purification system (≥18 MΩ, Milli-Q, Millipore) was used in all assays and all other reagents were of analytical reagent grade.

2.2. Apparatus

All electrochemical measurements were performed on a CHI660D electrochemical workstation (Shanghai Chenhua Instruments Co. Ltd., China) with a conventional three-electrode system composed of platinum wire as auxiliary, Ag/AgCl electrode as reference, and a 3-mm diameter glassy carbon electrode (GCE) as working electrode. The ECL measurements were carried out with a model MPI-A ECL analyzer (Xi'an Remax Electronic Science & Technology Co. Ltd., Xi'an, China). A UV–visible spectrophotometer (UV-2550, Shimadzu, Kyoto, Japan) was used to demonstrate features of the nanomaterials. Morphology and elemental mapping analysis of the prepared nanomaterial were characterized by the scanning electron microscope (SEM, SU-8010, Hitachi, Tokyo, Japan). Fluorescent PCR was performed in iCycler iQ Real-Time Detection System (Bio-Rad, Hercules, Calif.).

2.3. Synthesis of CuMn-CeO_2 nanomaterials

CuMn-CeO_2 were prepared according to previous method with a little modification (Liu et al., 2014). Firstly, added 500 mg Ce $(NO_3)_3{\cdot}6H_2O$ and 200 mg PVP into 28 mL ethylene glycol (EG) and then stirred for 30 min. Secondly, 1 mL $MnCl_2$ (20 mg mL^{-1}) and 1 mL $CuCl_2{\cdot}2H_2O$ (20 mg mL^{-1}) solution were mixed with the above solution, transferred into a Teflon-lined autoclave of 50 mL capacity and heated for 8 h at 180 °C. The prepared products were collected and washed with absolute alcohol and deionized water several times after cooling to room temperature. At last, the resultant products were dried at 60 °C. The synthetic procedure of CeO_2 was shown in Supporting information.

2.4. Preparation of CuMn-CeO_2-PEI-luminol-SP bioconjugates

The scheme of CuMn-CeO_2-PEI-luminol-SP bioconjugates (SP bioconjugates) preparation was shown in Fig. S1. Initially, 2 mg CuMn-CeO_2 was stirred with 1% polyethylenimine (PEI) for 4 h. Following, the mixture was centrifuged to acquire the PEI wrapped CuMn-CeO_2 (CuMn-CeO_2-PEI). Whereafter, 500 μL 12.5% GA and 1 mL 0.1 M luminol were added into the above-mentioned precipitate and stirred for 12 h at room temperature. After centrifugation, the obtained sediment (CuMn-CeO_2-PEI-luminol) was resuspended in 1 mL deionized water. Next, 20 μL SP (10 μM) was added into 200 μL NHS (10 mM) and EDC (40 mM) solution for 30 min to activate -COOH of the carboxylated SP. Subsequently, the above solution was mixed with 100 μL CuMn-CeO_2-PEI-luminol at 4 °C for 12 h to synthesize CuMn-CeO_2-PEI-luminol-SP bioconjugates. The centrifuged sediment was thoroughly rinsed to obtain the SP bioconjugates, dispersed in 0.1 M PBS (pH 7.4) and stored at 4 °C for further use.

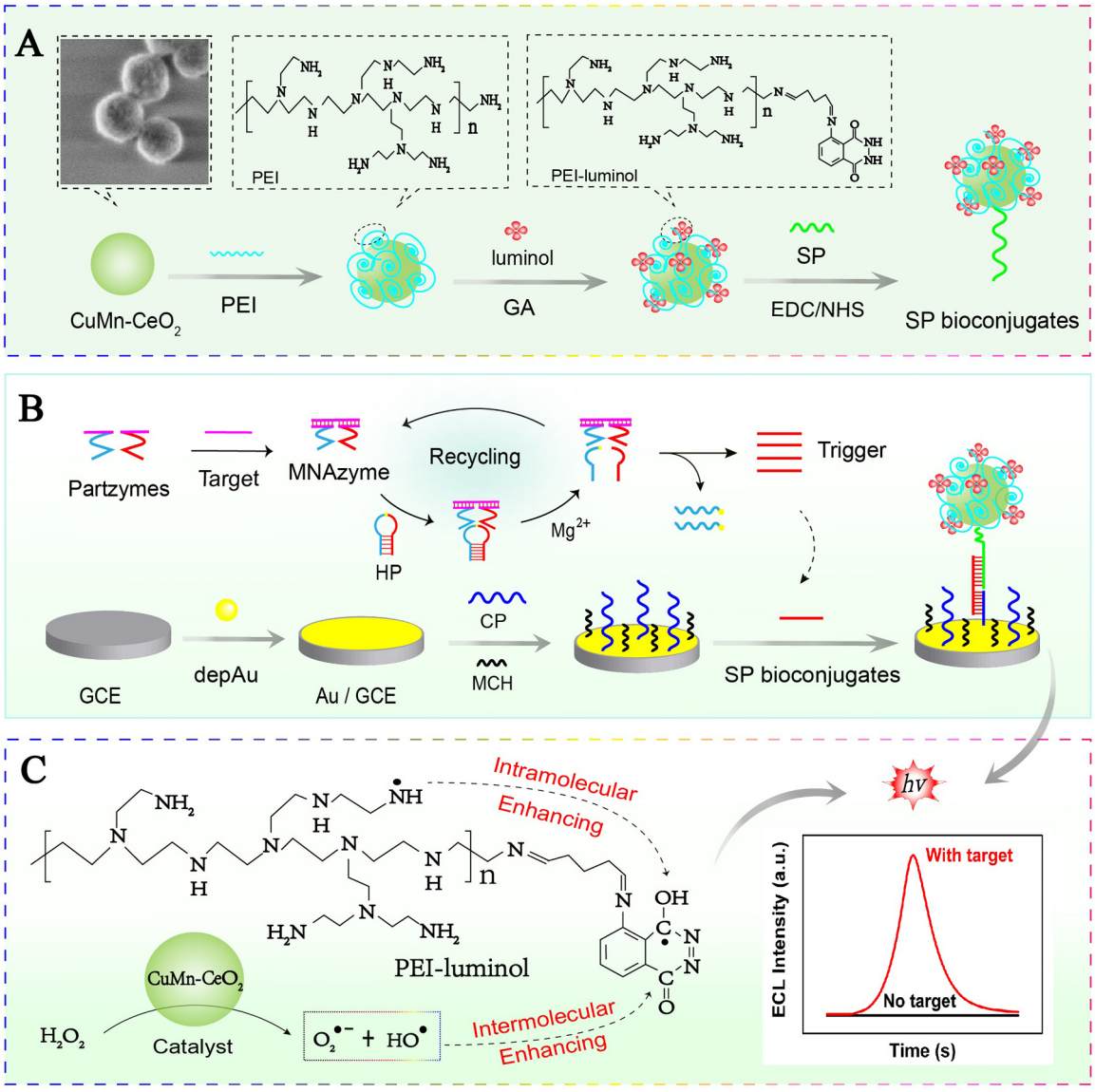

Scheme 1. Schematic illustration of novel self-enhanced CuMn-CeO_2-PEI-luminol and MNAzyme-mediated target-recycling-based ECL biosensor assay. (A) The preparation of self-enhanced CuMn-CeO_2-PEI-luminol-SP bioconjugates; (B) The process of MNAzyme-mediated target-recycling and fabrication of the ECL sensing platform; (C) The mechanism of the self-enhanced CuMn-CeO_2-PEI-luminol nanocomposites.

2.5. Polyacrylamide gel electrophoresis

The feasibility of the fabricated biosensor was evaluated by 8% native polyacrylamide gel electrophoresis (PAGE) in 1 × TBE buffer (89 mM Tris-boric acid, 2 mM EDTA, pH 8.3) at 90 V constant voltage for 45 min at room temperature. The gels were imaged using gel image system (Bio-Rad Laboratories, USA).

2.6. DNA extraction from GBS culture and clinical specimens

GBS strain was obtained from Microbiology Department of Chongqing Medical College, China. The pure GBS strain was grown in Luria-Bertani medium with constant shaking for 16 h at 37 °C. Then the culture was carefully washed in sterile deionized water by centrifugation at 12,000 rpm for 10 min and resuspended in 1 mL sterile deionized water. Next, 100 μL of the above dilution was plating onto plate count agar to get individual colonies. After incubating the plate at 37 °C for 24 h, the culture colonies were counted to estimate forming unit per milliliter (CFU mL^{-1}) on the plates. Then genomic DNA was extracted from 1 mL of different concentration cultures using the Bacterial Genomic DNA Extraction Kit according to the instruction and re-suspended in 50 μL of sterile deionized water.

The vaginal/anal samples of pregnant women for prenatal or intrapartum GBS screening were collected from The First Affiliated Hospital of Chongqing Medical University, China. *Group B Streptococus* Nucleic Aid Detection Kit (Fluorescent PCR) was used to directly extract genomic DNA from 1 mL of vaginal/anal lysates according to the instruction and resuspended in 50 μL of sterile deionized water. All the prepared DNA was stored at − 20 °C for further use.

2.7. Construction of the ECL sensing platform

A glassy carbon electrode (GCE, Φ = 3 mm) was firstly polished with 0.3 and 0.05 μm alumina to obtain mirror-like surface, followed by rinsing with deionized water and ethanol in ultrasonic bath and dried at room temperature. The pretreated GCE was immersed into 1% (w/w)

$HAuCl_4$ solution to obtain Au film by the electrochemical deposition under constant potential of − 0.2 V for 25 s. Subsequently, the formed Au modified GCE (Au/GCE) was incubated with 15 μL CP (1 μM) at 4 °C for 12 h. After immobilization of CP, 10 μL MCH (1 mM) solution was added to the electrode for 4 h at room temperature to cover the non-specific sites. Thus, the sensing platform was constructed successfully and depicted in Scheme 1B.

2.8. Target DNA detection protocol

MNAzyme mediated target-recycling amplification was carried out by mixing 2 μL partzyme A (1 μM), 2 μL partzyme B (1 μM), 2 μL HP (1 μM), and varying concentrations of target DNA in MNAzyme buffer to give a total volume of 20 μL, and the final concentrations of partzyme A, partzyme B and HP were 100 nM. Afterward, the mixtures were incubated at 37 °C for 90 min and then mixed with 20 μL SP bioconjugates for further reaction. In the next moment, 10 μL of resulted reaction mixture was added to the electrode surface and incubated at 37 °C for 30 min. Finally, in order to capture the ECL signal, the modified electrode was thoroughly cleaned with PBS (pH 7.4) and investigated by the MPI-A ECL analyzer in 4 mL 0.1 M PBS (pH 7.4) containing 5 mM H_2O_2 from 0 to 0.6 V at the scan rate of 100 mV s^{-1} with the voltage of the photomultiplier tube (PMT) at 800 V.

3. Results and discussion

3.1. Characterization of CuMn-CeO_2 and CuMn-CeO_2-PEI-luminol

The morphologies of CuMn-CeO_2 and CuMn-CeO_2-PEI-luminol were characterized by scanning electron microscope (SEM) (Fig. 1A-C). As shown in Fig. 1A, the CuMn-CeO_2 showed uniform-size nanospheres with an average diameter of 110 nm and the rough surfaces were observed from a close-up view of SEM image (Fig. 1B). PEI-luminol with irregular morphology was shown in Fig. S2A. After modifying with PEI-luminol, the size of CuMn-CeO_2-PEI-luminol increased to about 200 nm and the some caves on uneven surface were observed (Fig. 1C). The corresponding SEM of CeO_2-PEI-luminol was displayed in Fig. S2B and C. We also noticed that SEM of CeO_2-PEI-luminol and CuMn-CeO_2-PEI-luminol were similar. The above results showed that PEI-luminol had successfully modified on CuMn-CeO_2 and CeO_2. In addition, differential scanning calorimetry (DSC) experiment was also performed for CuMn-CeO_2 and the result was displayed in Fig. S3.

Besides, elemental mapping analysis using energy dispersive spectroscopy (EDS) was conducted on a single CuMn-CeO_2 (Fig. 1D) to verify the occurrence of homogeneous distributions of O, Ce, Mn and Cu (Fig. 1E-H), respectively. The results showed that Cu/Mn bimetallic elements were successfully doped into CeO_2. We also carried out UV–vis absorption spectrum experiment to investigate whether CuMn-CeO_2 and CuMn-CeO_2-PEI-luminol were successfully synthesized (Fig. S4). The results were consistent with the reported literature (Khan et al., 2017; Nair et al., 2018).

3.2. Feasibility of the ECL biosensing strategy

The feasibility of MNAzyme-mediated target-recycling amplification based ECL biosensor for target DNA detection was verified by 8% native polyacrylamide gel electrophoresis (PAGE) (Fig. S5). Control experiments were carried out to contrast the ECL intensity for the fabricated biosensor system at different experimental conditions (Fig. 2). The control experiments, excluding partzyme A, partzyme B, HP, CP, SP bioconjugates and target DNA respectively, showed weak signals around 500 au. In the absence of target DNA (curve a), partzyme A (curve b), partzyme B (curve c) or HP (curve d), almost no active MNAzyme was formed, which could not trigger hybridization reaction on the electrode. In addition, although the active MNAzyme existed, hybridization reaction could not be triggered in the absence of CP and SP bioconjugates due to the lack of CP (curve e) and SP bioconjugates (curve f) (Fig. 2B). However, a high ECL signal about 4500 au was obtained in the presence of target DNA (curve g) because numerous self-enhanced SP bioconjugates were specifically immobilized on the electrode surface (Fig. 2A). These results clearly demonstrated the feasibility of the developed ECL biosensing method for highly sensitive detection of target DNA. In addition, electrochemical impedance spectroscopy (EIS) was also conducted to characterize the successful stepwise assembling process of the ECL biosensor, the experimental results were shown in Fig. S6, indicating that the ECL biosensor was successfully constructed.

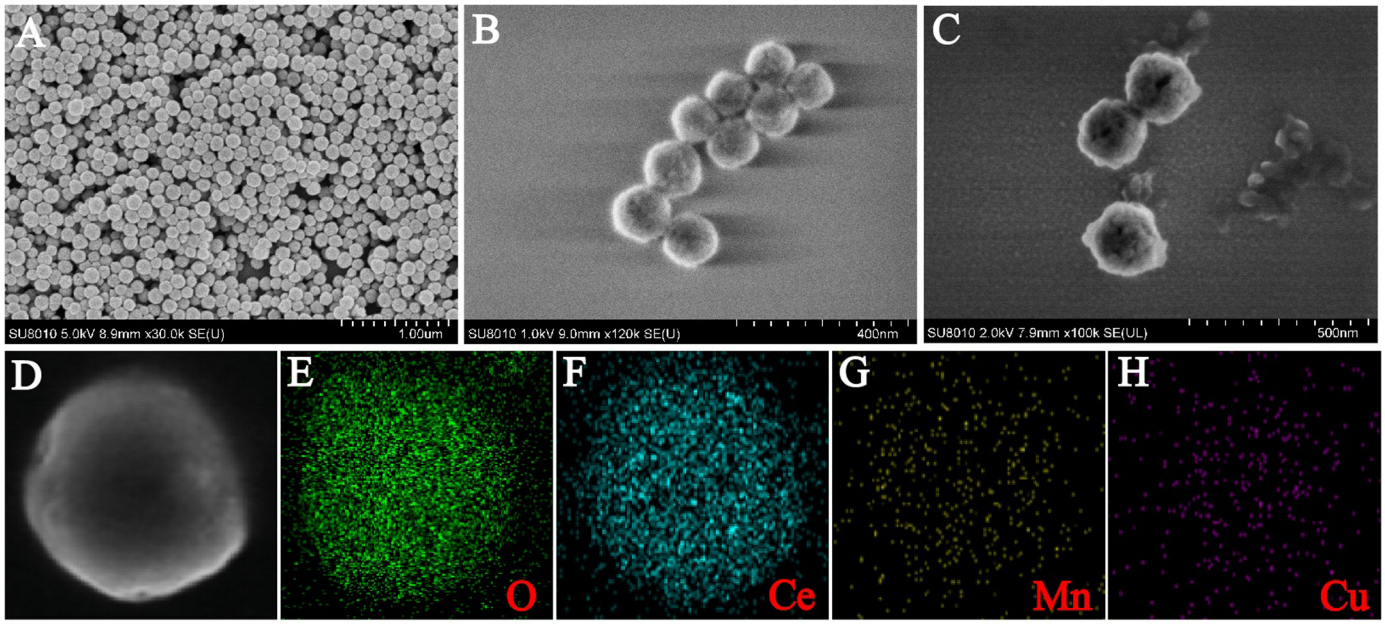

Fig. 1. SEM images with different magnifications of the CuMn-CeO_2 (A, B), CuMn-CeO_2-PEI-luminol (C). EDS-mapping images of an individual CuMn-CeO_2 nanosphere (D): O (green, E), Ce (blue, F), Mn (yellow, G) and Cu (purple, H).

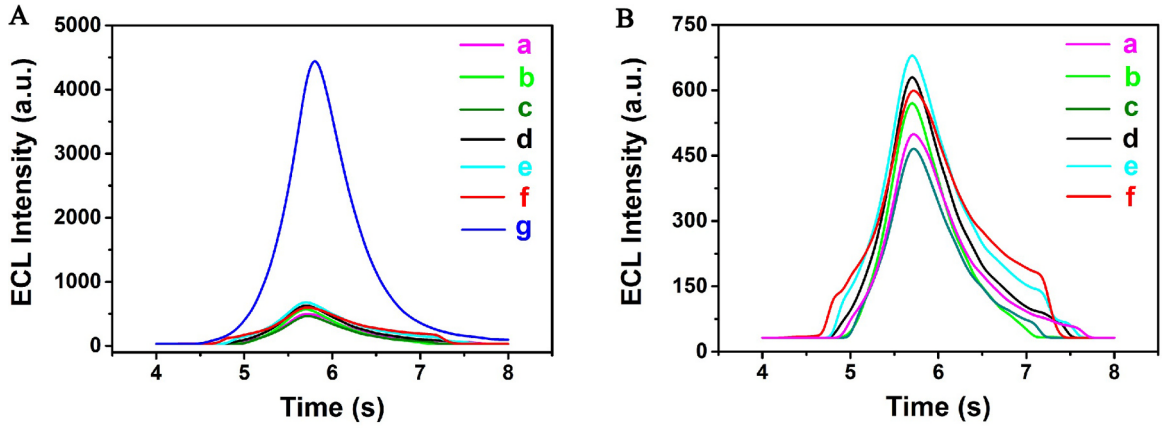

Fig. 2. (A) ECL intensities of the fabricated biosensor at different experimental conditions: (a) no target DNA, (b) no partzyme A, (c) no partzyme B, (d) no HP, (e) no CP, (f) no SP bioconjugates, (g) including all the components. (B) was the amplified illustration of A.

3.3. Mechanism of the novel self-enhanced CuMn-CeO_2-PEI-luminol bioconjugates

The effect of PEI on the ECL of luminol was explored in Supporting information. The results indicated that PEI as co-reactant of luminol could greatly amplify the ECL signal of luminol (Fig. S7). And the effect of PEI associated with Cu/Mn double-doped CeO_2 nanocomposites on the ECL of luminol was firstly investigated. Moreover, H_2O_2 as the most commonly used co-reactant of luminol and the ECL signal of luminol-H_2O_2 system could be amplified by the catalysis of metal oxide nanoparticles, Cu/Mn double-doped CeO_2. Herein, we also investigated the effect of different metal oxide nanoparticles on the ECL of luminol-H_2O_2 system. As shown in Fig. 3A, three different ECL biosensor were fabricated using same modified method with different bioconjugates. The bioconjugates were (a) PEI-luminol, (b) CeO_2-PEI-luminol and (c) CuMn-CeO_2-PEI-luminol respectively. The three kinds of ECL biosensors were performed under same detecting condition with same concentration analyte (1 pM of target DNA). The ECL intensities obtained from the three ECL biosensors were 2267 au, 3515 au and 5137 au, respectively. Obviously, it could be seen that the value obtained from the ECL biosensor based on CuMn-CeO_2-PEI-luminol bioconjugates was about 1.5 times that of CeO_2-PEI-luminol and 2.5 times that of PEI-luminol. The reasons could be attributed to that, firstly, PEI as an intramolecular co-reactant of luminol shortened electron transfer distance and reduced the energy loss of co-reaction between luminol and PEI, which could further strengthen the ECL signal. Secondly, the high catalytic activity of CuMn-CeO_2 toward H_2O_2 oxidation played an important role in the signal amplification of luminol-H_2O_2 ECL luminous system as well. The results indicated that the intramolecular self-enhanced luminophore PEI-luminol strengthened the ECL signal bravely, and the double doped CuMn-CeO_2 improved the catalytic performance of CeO_2 toward H_2O_2. The possible mechanisms were described in Fig. 3B.

3.4. Analytical performance of biosensor

In order to efficiently and sensitively detect target DNA with this developed ECL biosensor, five key parameters were optimized in Fig. S8. Under the optimal analytical conditions, the sensitivity of this proposed assay was investigated by evaluating the dependence of ECL intensity upon the concentration of target DNA. As displayed in Fig. 4A, the ECL intensities increased as the increase of target DNA concentrations in the range from 0.1 fM to 1 nM (from a to h). Fig. 4B exhibited the calibration plot of ECL intensity *vs* logarithm of target DNA concentration with a linear regression equation of $I = 998.7 \lg c + 1539.1$ (where I stands for ECL intensity and c stands for the concentration of target DNA), with the square of correlation coefficient (R^2) of 0.9964. The detection limit was estimated at 63 aM corresponding to three times the average standard deviation of the blank signal.

Furthermore, the detection limit for target DNA of the proposed method was compared with the reported methods, it showed high sensitivity with about 2–7 orders of magnitude improvement (Table S2). The ultra-sensitivity was attributed to the intramolecular and intermolecular self-enhanced CuMn-CeO_2-PEI-luminol bioconjugates. The target-driven MNAzyme system was not only used to realize the circulation of GBS nucleic acid sequence, but also improve the specificity of GBS detection in this strategy.

3.5. Specificity, reproducibility, stability and recovery experiments of the strategy

Specificity, reproducibility and stability were monitored in Supporting information (Fig. S9) for their vital roles in sensing system. And to evaluate the capability of the designed ECL biosensor in complex sample matrix, we employed salmon sperm DNA as a model. The salmon sperm DNA was first denatured at 95 °C for 5 min and chilled on ice for 10 min, varied amounts of target DNA were mixed with the samples and tested in this biosensor. Despite the presence of 200 pg/mL salmon sperm DNA, the analysis results of 1 pM, 10 pM and 100 pM target DNA demonstrated the recoveries of 103.3%, 105.6%, 107.0%, respectively (Table 1). It was implied that the analytical performance of the proposed biosensor was not compromised in complex mixtures because of steadily design.

3.6. Real sample analysis

To evaluate the practical applicability in real sample analysis, the established ECL biosensor was employed to directly detect the specific sequence of genomic DNA which extracted from serially diluted GBS without PCR. As shown in Fig. 4C, the ECL intensities were proportional with the genomic DNA concentration in the range of 10^3-5×10^7 CFU mL^{-1} and the GBS detection limit was calculated to be about 500 CFU mL^{-1} according to this work. The results also confirmed no loss of analytical performance of the biosensor for detection of enormous and complicated genomic DNA in real samples.

The proposed strategy was further applied to evaluate the practical applicability in clinical samples by directly detecting GBS from 51 clinical vaginal/anal swabs of women who were 34–37 weeks of pregnancy. Among the 51 vaginal/anal lysates, 26 were identified as positive and 25 identified as negative by this strategy with a positive threshold (PT) of 380 au, which was defined as three times of the standard deviation of 5 blank samples. At the same time, these samples were detected with commercial fluorescent PCR assay (Ct ≤ 38, positive; Ct > 45, negative;

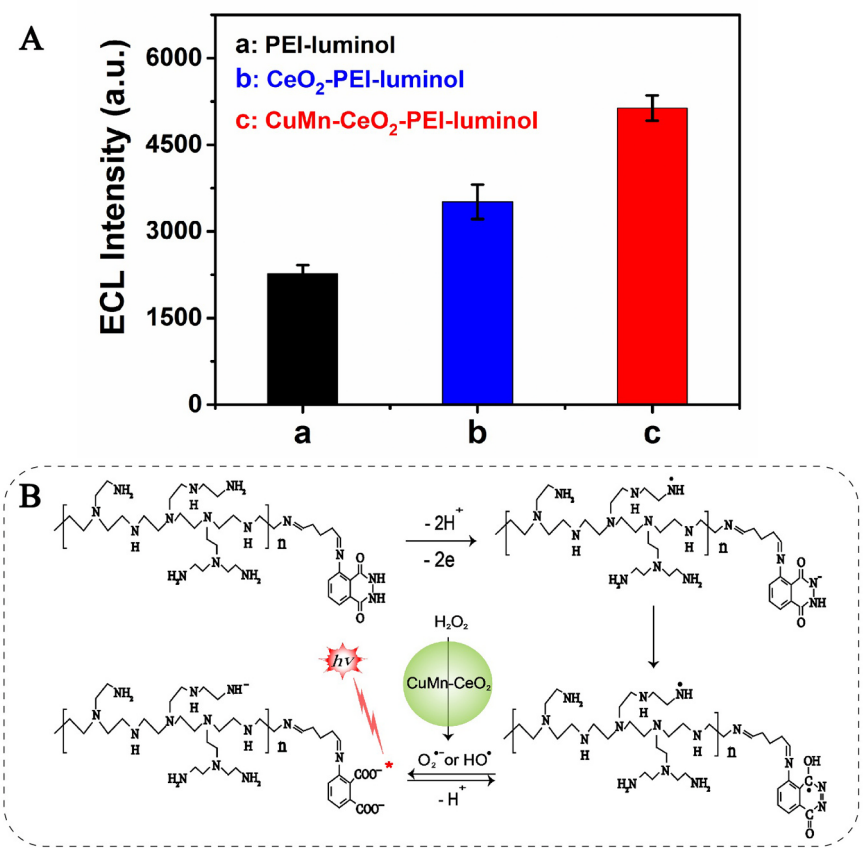

Fig. 3. (A) Comparison of catalytic efficiency between (a) PEI-luminol, (b) CeO_2-PEI-luminol and (c) CuMn-CeO_2-PEI-luminol on the electrode in 0.1 M PBS containing 5 mM H_2O_2 at the scan rate of 100 mV s^{-1}. (B) Mechanisms of PEI and CuMn-CeO_2 nanocomposites enhanced ECL signal of luminol.

38 < Ct ≤ 45, critical value), displaying 100% of both negative and positive predict values. Results showed that the proposed method agreed with the fluorescent PCR completely (Fig. 4D). When comparing the results of two assays for the 26 GBS positive samples using regression analysis, the cycle threshold (Ct) values obtained with the commercial fluorescent PCR assay *vs* that of ECL intensities obtained with the established biosensor gave a R^2 value of 0.991, which still further confirming complete agreement of the two methods (Fig. S10). Furthermore, the low detection limit was calculated to be 320 copies in this proposed strategy which was lower than that of fluorescent PCR assay (1000 copies). Surprisingly, two clinical vaginal/anal swabs with extremely low GBS content could be identified accurately which displayed higher Ct between 38 and 45. These results showed strong evidence of the proposed method held comparable specificity and sensitivity with fluorescent PCR method for GBS screening in clinical vaginal/anal swabs. What's more, the efficient analytical performance was implemented without the need of complicated biologic enzymes, sophisticated instruments, and cascade signal amplification procedures, exhibiting practical application potential toward clinical diagnosis.

4. Conclusion

In summary, a novel and pragmatic electrochemiluminescence (ECL) biosensing method was developed for ultrasensitive and specific detection of *Group B Streptococci* (GBS) by combining self-enhanced luminol complex functionalized CuMn-CeO_2 (CuMn-CeO_2-PEI-luminol) with MNAzyme-mediated target-recycling amplification. The ultrasensitivity achieved for detection of ECL signals attributed to the intramolecular enhancing of efficient PEI-luminol luminophore and the intermolecular enhancing of highly catalytic CuMn-CeO_2 toward H_2O_2 oxidation. Besides, the target-driven MNAzyme system was not only realize the circulation of GBS nucleic acid sequence, but also improve the specificity of GBS detection. Thus, the developed biosensing method might become a pragmatic ECL platform for ultrasensitive and specific detection of GBS in clinical vaginal/anal swabs. However, the MNAzyme-mediated amplification reaction and hybridization reaction were carried out separately in this work, which extended the detection time. In view of this defect, we would focus on improving the disadvantage in future work so as to shorten detection time.

CRediT authorship contribution statement

Jiaji Ling: Conceptualization, Methodology, Software, Investigation, Data curation, Writing - original draft. **Min Zhao:** Methodology, Software, Investigation, Project administration, Writing - review & editing. **Fengjiao Chen:** Formal analysis, Software, Validation. **Xiaoyan Zhou:** Conceptualization, Data curation, Validation. **Xiaosong Li:** Resources, Software. **Shijia Ding:** Supervision, Methodology, Data curation. **Hua Tang:** Funding acquisition, Supervision, Data curation.

Acknowledgment

This study was supported by the Program for Innovation Team of Higher Education in Chongqing (CXTDX201601015), the National Natural Science Foundation of China (81873980 and 21804015), the Natural Science Foundation Project of CQ CSTC (cstc2018jcyjAX0206), the China Postdoctoral Science Foundation (2017M622979),

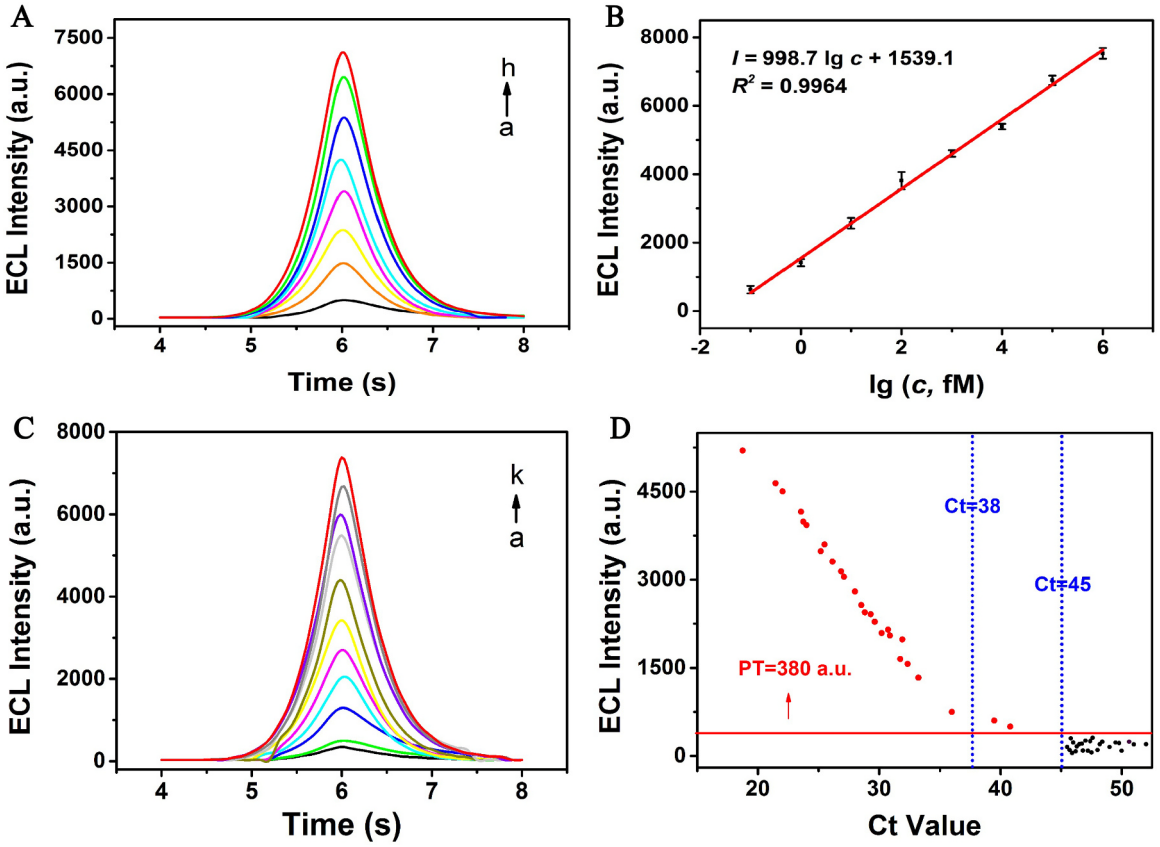

Fig. 4. (A) ECL intensity for detection of target DNA at 0.1 fM, 1 fM, 10 fM, 100 fM, 1 pM, 10 pM, 100 pM and 1 nM (from a to h). (B) The calibration curve of ECL intensity versus target DNA at 0.1 fM, 1 fM, 10 fM, 100 fM, 1 pM, 10 pM, 100 pM and 1 nM. Error bars are standard derivation obtained from three independent experiments. (C) Typical ECL intensity curves of the designed method responding to 0, 10^3 CFU mL^{-1}, 5×10^3 CFU mL^{-1}, 10^4 CFU mL^{-1}, 5×10^4 CFU mL^{-1}, 10^5 CFU mL^{-1}, 5×10^5 CFU mL^{-1}, 10^6 CFU mL^{-1}, 5×10^6 CFU mL^{-1}, 10^7 CFU mL^{-1}, 5×10^7 CFU mL^{-1} of GBS (from a to k), respectively. (D) Comparison between the ECL intensity of proposed biosensor and Ct value of fluorescent PCR assay for 51 clinical samples. Red dots represented 26 positive clinical samples and black dots represented 25 negative clinical samples.

Table 1
Recovery results of target DNA in salmon sperm DNA.

Sample	Spiking Value (pM)	Assayed Value (pM)	Recovery (%)	SD[a] (%)	CV[b] (%)
1	1	1.03	103.3	9.2	1.6
2	10	10.56	105.6	12.6	1.3
3	100	106.98	107.0	8.5	1.5

[a] SD, standard deviation.
[b] CV, coefficient of variation.

Chongqing Postdoctoral Science Special Foundation (XmT2018073) and the Leading Talent Program of CQCSTC (CSTCCXLJRC201719).

Declaration of interests

None.

Appendix A. Supporting information

Supplementary data associated with this article can be found in the online version at https://doi.org/10.1016/j.bios.2018.12.012.

References

Danis, A.S., Potts, K.P., Perry, S.C., Mauzeroll, J., 2018. Anal. Chem. 90 (12), 7377–7382.
Hao, N., Wang, K., 2016. Anal. Bioanal. Chem. 408 (25), 7035–7048.
Jiang, X., Wang, H., Wang, H., Zhuo, Y., Yuan, R., Chai, Y., 2016. Nanoscale 8 (15), 8017–8023.
Johri, A.K., Paoletti, L.C., Glaser, P., Dua, M., Sharma, P.K., Grandi, G., Rappuoli, R., 2006. Nat. Rev. Microbiol. 4 (12), 932–942.
Ke, H., Zhang, X., Huang, C., Jia, N., 2018. Biosens. Bioelectron. 103, 62–68.
Khan, M.A.M., Khan, W., Ahamed, M., Alhazaa, A.N., 2017. Sci. Rep. 7 (1), 12560.
Kuo, C.C., Lan, W.J., Chen, C.H., 2014. Nanoscale 6 (1), 334–341.
Liang, J., Li, M., Lu, Y., Yao, H., Liu, H., 2018. Biosens. Bioelectron. 118, 44–50.
Liu, W., Liu, X., Feng, L., Guo, J., Xie, A., Wang, S., Zhang, J., Yang, Y., 2014. Nanoscale 6 (18), 10693–10700.
Mandal, B., Mondal, A., Ray, S.S., Kundu, A., 2016. Dalton Trans. 45 (4), 1679–1692.
Mao, L., Yuan, R., Chai, Y., Zhuo, Y., Xiang, Y., 2011. Biosens. Bioelectron. 26 (10), 4204–4208.
Mayer, M., Takegami, S., Neumeier, M., Rink, S., Jacobi von Wangelin, A., Schulte, S., Vollmer, M., Griesbeck, A.G., Duerkop, A., Baeumner, A.J., 2018. Angew. Chem. Int. Ed. 57 (2), 408–411.
Mokany, E., Bone, S.M., Young, P.E., Doan, T.B., Todd, A.V., 2010. J. Am. Chem. Soc. 132 (3), 1051–1059.
Nair, S., Nagarajappa, G.B., Pandey, K.K., 2018. J. Photochem. Photobiol. B 183, 1–10.
Stroppa, D.G., Dalmaschio, C.J., Houben, L., Barthel, J., Montoro, L.A., Leite, E.R., Ramirez, A.J., 2014. Chemistry 20 (21), 6288–6293.
Wang, F., Elbaz, J., Teller, C., Willner, I., 2011. Angew. Chem. Int. Ed. 50 (1), 295–299.
Wang, F., Li, W., Feng, X., Liu, D., Zhang, Y., 2016a. Chem. Sci. 7 (3), 1867–1873.
Wang, H., Yuan, Y., Chai, Y., Yuan, R., 2015. Biosens. Bioelectron. 68, 72–77.
Wang, J.X., Zhuo, Y., Zhou, Y., Wang, H.J., Yuan, R., Chai, Y.Q., 2016b. ACS Appl. Mater. Interfaces 8 (20), 12968–12975.
Wang, T., Wang, D., Padelford, J.W., Jiang, J., Wang, G., 2016c. J. Am. Chem. Soc. 138 (20), 6380–6383.
Xu, L., Wang, J., 2012. Environ. Sci. Technol. 46 (18), 10145–10153.
Yan, M., Bai, W., Zhu, C., Huang, Y., Yan, J., Chen, A., 2016. Biosens. Bioelectron. 77, 613–623.
Yang, J., Cho, M., Lee, Y., 2016. Biosens. Bioelectron. 75, 15–22.
Zhang, D.Y., Turberfield, A.J., Yurke, B., Winfree, E., 2007. Science 318 (5853), 1121–1125.
Zhang, H., Guo, Z., Dong, H., Chen, H., Cai, C., 2017. Analyst 142 (11), 2013–2019.
Zhang, Y., Li, X., Xu, Z., Chai, Y., Wang, H., Yuan, R., 2018. Chem. Commun. 54 (72), 10148–10151.
Zhao, J., Lu, C., He, X., Zhang, X., Zhang, W., Zhang, X., 2015. ACS Appl. Mater. Interfaces 7 (4), 2607–2615.
Zhao, M., Chen, A.Y., Huang, D., Chai, Y.Q., Zhuo, Y., Yuan, R., 2017. Anal. Chem. 89 (16), 8335–8342.
Zhao, M., Chen, A.Y., Huang, D., Zhuo, Y., Chai, Y.Q., Yuan, R., 2016. Anal. Chem. 88 (23), 11527–11532.
Zhou, Y., Chen, S., Luo, X., Chai, Y., Yuan, R., 2018. Anal. Chem. 90 (16), 10024–10030.